VERIFICATION OF NUMERICAL SOLUTION OF TWO-DIMENSIONAL REACTIVE FLOW IN ROCKET ENGINE NOZZLES

Luciano Kiyoshi Araki, lucaraki@demec.ufpr.br
Programa de Pós-Graduação em Métodos Numéricos em Engenharia – UFPR, Curitiba – PR, Brazil

Carlos Henrique Marchi, marchi@demec.ufpr.br
Department of Mechanical Engineering, Federal University of Paraná, Curitiba, PR, Brazil

Abstract. *Two-dimensional mathematical models for LOX-LH_2 reactive flow are solved for two geometries – a conical and a parabolical ones. Five different physical models are considered: two one-species ones (which include a single-specie gas with constant or with variable properties) and three mixture of gases ones (frozen, equilibrium and non-equilibrium flows). Associated to these three models, different chemical reaction schemes are studied, in order to provide the influence of the number of species and the number of chemical reaction equations on results. Therefore, numerical solutions are obtained for different grid sizes, so as to afford the numerical error estimate, by GCI error estimator. At the mathematical model, temperature is used as unknown at energy equation and velocity is obtained for all speed flows, from almost null values (at the flow starting-point) to supersonic ones. For all the analysis, a non-orthogonal finite volume program, called Mach2D 6.0 and written in Fortran 95 language, was implemented, taking into account second order scheme for variables and co-located grid arrangement. For the conical geometry, both pressure and two-dimensional discharge coefficient values for one-species flow were compared to experimental values and the analytical solution, respectively, showing good concordance. For the parabolical geometry, first and second order schemes were compared for grids as refined as 360x96 volumes and the GCI estimates were obtained, showing differences as high as four-orders of magnitude for global variables of interest.*

Keywords*: Finite Volume Method, Non-Orthogonal Grid, Equilibrium flow, Non-Equilibrium Flow, Error Estimators.*

1. INTRODUCTION

The effort to increase reliability in rocket engines should span the entire program spectrum from conceptual design through production. The reliability effort can basically be split into three parts: prevention of failures, process assessment and control, and monitoring of performance (Huzel and Huang, 1992). One possible reason for wall material failure is its high temperatures and this is the explanation for studying the heat transfer overall the rocket engine nozzle. Heat is transmitted to all internal hardware surfaces exposed to hot gases, namely the injector face, the chamber and nozzle walls. Only 0.5 to 5% of the total energy generated in the gas is transferred as heat to the chamber walls (Sutton and Biblarz, 2001). To study the heat transfer from hot reaction gas products to the rocket walls, however, firstly it is necessary to define the reaction gas products flow features. Because of this, the focus of this work is the reaction gas products flow, in order to provide a deeper knowledge of the influence of both chemical and physical reaction schemes on the reaction gas products for a non-viscous two-dimensional flow.

Different physical and chemical schemes are used. Five two-dimensional physical models are compared in this work: one-species gas with constant properties, one-species gas with variable properties, frozen, equilibrium and non-equilibrium flows. Otherwise, for frozen, equilibrium and non-equilibrium flows, which include multi-species flows, chemical schemes are also considered. Differently from commonly used, the energy equation is based on temperature and the velocity is obtained for the whole flow (from subsonic to supersonic regimes). Nine different chemical reaction schemes for reaction gas products flow are presented, for frozen and equilibrium flows; these chemical reaction schemes are the same ones presented by Marchi *et al*. (2005) and Araki and Marchi (2006), including from 3 to 8 chemical species and from 0 to 18 chemical reaction equations.

All the models have been implemented using Compaq Visual Fortran 6.6.0. The implemented code, called Mach2D 6.0, was run at a PC Pentium IV, 3400 MHz, with 4.0 GB RAM. Pressure results for air flow are compared to those ones obtained by Back *et al*. (1965), in order to validate the code. For a second geometry, a parabolic one, numerical error estimates, related to all results and based on GCI estimative (Roache, 1994), using the methodology presented by Marchi (2001), are also made.

2. MATHEMATICAL MODEL

The basic principles involved in rocket propulsion science are essentially those ones of mechanics, thermodynamics and chemistry (Sutton and Biblarz, 2001). In regeneratively cooled rocket engines, the whole thrust mechanism can be divided up into three different (but coupled) problems, for which there are independent mathematical (and numerical) models (Fröhlich *et al*., 1993; Habiballah *et al*., 1998; Marchi *et al*., 2004): (1) the reaction gas products (combustion gases mixture) flow through the thrust chamber; (2) the heat conduction from hot gases to the coolant; and (3) the

coolant flow through the regenerative cooling system. The focus of this work is, however, the reaction gas products flow, which is modelled by the following equations: mass conservation equation, two-dimensional Euler ones (for axial and radial directions), energy equation, and a state relation:

$$\frac{\partial}{\partial z}(\rho u) + \frac{1}{r}\frac{\partial}{\partial r}(r \rho v) = 0 \tag{1}$$

$$\frac{\partial}{\partial z}(\rho u u) + \frac{1}{r}\frac{\partial}{\partial r}(r \rho v u) = -\frac{\partial P}{\partial z} \tag{2}$$

$$\frac{\partial}{\partial z}(\rho u v) + \frac{1}{r}\frac{\partial}{\partial r}(r \rho v v) = -\frac{\partial P}{\partial r} \tag{3}$$

$$\frac{\partial}{\partial z}(\rho u T) + \frac{1}{r}\frac{\partial}{\partial r}(r \rho v T) = \frac{1}{c_p}\left[\nabla(P\vec{V}) - P\nabla\vec{V}\right] + S_{eq/tf} \tag{4}$$

$$P = \rho R T \tag{5}$$

where: ρ, u, v, P e T are the five dependent variables, which correspond to density, axial velocity, radial velocity, pressure and temperature, respectively; z and r are related to the axial and the radial directions, in this order; c_p is the frozen specific heat; R is the gas mixture constant; $\vec{V}$ is the velocity vector; and $S_{eq/tf}$ is the chemical source term, which is evaluated by:

$$S_{eq/tf} = -\frac{1}{c_p}\left[\sum_{i=1}^{N} h_i \frac{\partial}{\partial z}(\rho u Y_i) - \sum_{i=1}^{N} h_i \frac{1}{r}\frac{\partial}{\partial r}(r \rho v Y_i)\right] \tag{6a}$$

for local equilibrium flow model; and by

$$S_{eq/tf} = -\frac{1}{c_p}\sum_{i=1}^{N} h_i \dot{w}_i \tag{6b}$$

for non-equilibrium flow model, in which: N is the total number of chemical species; Y_i, h_i and $\dot{w}_i$ are, in this order, the mass fraction, the enthalpy and the generation rate for a given chemical species i. It must be noted that for the other physical models (one-species gas and frozen flow ones), this term is null. Considering the non-equilibrium flow, another equation must be taken into account: the species continuity equation,

$$\frac{\partial}{\partial z}(\rho u Y_i) + \frac{1}{r}\frac{\partial}{\partial r}(r \rho v Y_i) = \dot{w}_i \tag{7}$$

Chemical reactions schemes used in this work for frozen and local equilibrium flows are summarized in Tab. 1. For non-equilibrium one, only six and eight reaction scheme models were considered, being the frozen/equilibrium chemical model 3 split into two: models 31 and 32, which differs from each other by forward reaction constants). These are the same chemical reaction schemes used before by Marchi *et al*. (2005) and Araki and Marchi (2006), which present, in this order, the thermochemical properties for oxygen/hydrogen reaction schemes and the complete one-dimensional problem.

3. NUMERICAL MODEL

The presented mathematical model for reaction gas products is discretized using finite volume method, appropriated for non-orthogonal geometries (Maliska, 1995). The domain is divided in *Nx* control volumes in axial direction *z* and in *Ny* volumes in radial direction *r*, in which the differential equations are integrated. A co-located grid arrangement, appropriated for all speed flows is used (Marchi and Maliska, 1994), associated with a second-order discretization scheme (CDS), with deferred correction (Ferziger and Perić, 2001). The systems of algebraic equations obtained are solved by MSI (*Modified Strong Implicit*) method (Schneider and Zedan, 1981).

Pressure and velocity are coupled by SIMPLEC algorithm (Van Doormaal and Raithby, 1984), in order to convert the mass equation in a pressure (or better, in a pressure-correction) one. So, the mass conservation equation, Eq. (1), is

used for determination of a pressure-correction (P'). The axial and radial velocity components, (u) and (v), are obtained from the Euler equations, Eqs. (2) and (3), and the energy equation, Eq. (4), is taken for temperature (T) determination. Density (ρ) is gotten from the state equation, Eq. (5), while Eq. (7) is also needed for non-equilibrium flow. It must be noted that axial velocity (u) is evaluated from very reduced values (near null values) until supersonic ones, and not only for supersonic values, as commonly found in literature.

An algorithm for the reactive two-dimensional reaction gas products flow is presented in the following.

Table 1. Chemical reaction schemes implemented in Mach2D 6.0 code.

Model	*L*	*N*	Species	Observations
0	0	3	H_2O, O_2, H_2	Ideal model
1	1	3	H_2O, O_2, H_2	–
2	2	4	H_2O, O_2, H_2, OH	–
3	4	6	H_2O, O_2, H_2, OH, O, H	4 reactions with 3rd body – Barros *et al*. (1990) and Smith *et al*. (1987)
4	4	6	H_2O, O_2, H_2, OH, O, H	4 reactions – Svehla (1964)
5	8	6	H_2O, O_2, H_2, OH, O, H	8 reactions (4 with 3rd body) – Barros *et al*. (1990)
7	8	6	H_2O, O_2, H_2, OH, O, H	8 reactions (4 with 3rd body) – Smith *et al*. (1987)
10	6	8	H_2O, O_2, H_2, OH, O, H, HO_2, H_2O_2	4 reactions from model 3 and 2 from Kee *et al*. (1990) – all the reactions including 3rd body
9	18	8	H_2O, O_2, H_2, OH, O, H, HO_2, H_2O_2	18 reactions (5 with 3rd body) – Kee *et al*. (1990)

Algorithm:

1. Data reading, grid generation and evaluation of metrics.
2. Estimation of all variables in an instant $t+\Delta t$ (time, however, is used only as a relaxation parameter).
3. Estimation of the inlet pressure and the inlet temperature.
4. Definition of the constant-pressure specific heat.
5. Coefficients calculation for the algebraic system (by discretization) of the axial momentum equation and solution of this system by MSI for the velocity u.
6. Coefficients calculation for the algebraic system (by discretization) of the axial momentum equation and solution of this system by MSI for the velocity v.
7. Coefficients calculation for the algebraic system (by discretization) of the energy equation and solution by MSI for temperature T.
8. Calculation of density (both, inside the control volumes and at their faces).
9. Calculation of SIMPLEC coefficients.
10. Estimation of face velocities.
11. Coefficients calculation for the algebraic system (by discretization) of the mass equation and solution by MSI for pressure correction P'.
12. Correction of nodal pressures, face and nodal densities and face and nodal velocities by pressure correction P'.
13. Return to item 11 until the achievement of the desired number of iterations.
14. In case of non-equilibrium flow model, the mass fractions Y_i should be obtained by the solution of an algebraic system using the MSI method.
15. Return to item 2, until the achievement of the desired number of iterations or until the satisfaction of a certain criterion.
16. Post-processing.

4. DEFINITION OF THE PROBLEM

The boundary conditions adopted for the combustion gases flow, shown in Fig. 1, are:

- Entrance conditions: Temperature (T) and pressure (P) are functions of stagnation parameters; the chemical mixture composition, given by mass fractions (Y_i), is obtained from local data (temperature and pressure); this is not necessary for one-species models. The entrance axial velocity (u) is obtained from a linear extrapolation from the values obtained for internal flow. The radial velocity (v) is taken as null.
- Nozzle walls: Adiabatic.
- Exit conditions: For supersonic flows in nozzles, no exit boundary conditions are required; for the implementation of a numerical model, however, exit boundary conditions are needed. Because of this, temperature (T), axial and radial velocities (u and v), pressure (P) and mass fractions (Y_i) are obtained by linear extrapolation from internal control volumes.
- Line symmetry: Symmetry conditions for all variables; null radial velocity.

For all the simulations made, two different geometries were chosen: the first one is presented by Back *et al*. (1965); the second one is a parabolic nozzle. Both nozzles are presented in Fig. 2.

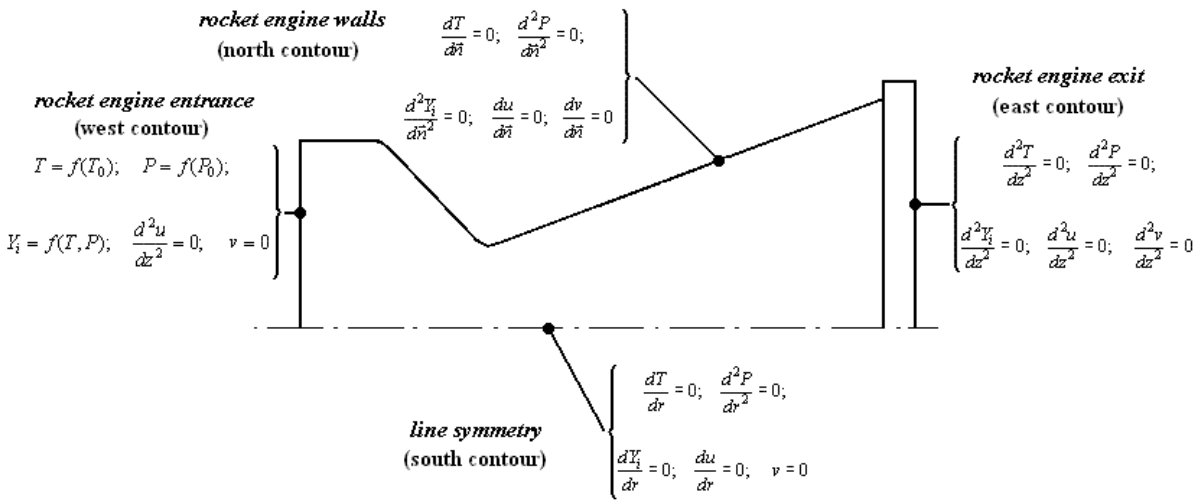

Figure 1. Boundary conditions for the reaction gas products flow.

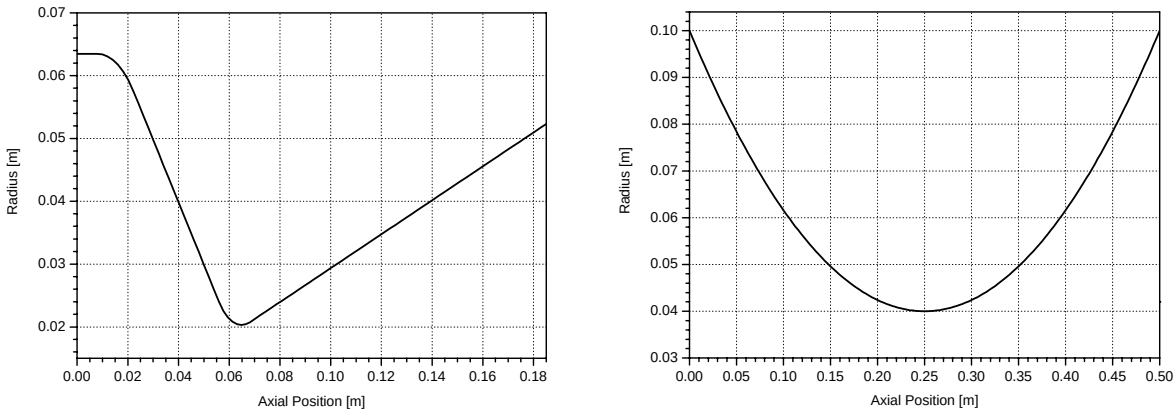

(a) (b)

Figure 2. Rocket engine profiles: (a) Geometry from Back *et al*. (1965). (b) Parabolic geometry.

The nozzle discharge coefficient (C_d) is defined as the ratio between experimental mass flux and the theoretical one, given by

$$C_d = \frac{\dot{m}_{\text{experimental}}}{\dot{m}_{\text{theoretical}}} \tag{8}$$

where the mass flux ($\dot{m}$) is obtained by the product of density, local velocity (u) and transversal section area (S):

$$\dot{m} = \int_{S_{exit}} \rho\, u\, dS \tag{9}$$

Another parameters of interest are the thrust (F), for vacuum conditions, and the thrust-chamber specific impulse (I_s), defined as:

$$F = \int_{S_{exit}} \rho\ u\ u\, dS \tag{10}$$

$$I_s = \frac{\int_0^{t_q} F\, dt}{g \int_0^{t_q} \dot{m}_p\, dt} \tag{11}$$

where g is the gravity acceleration, $\dot{m}_p$ is the propellant mass flux and t_q is the burn-out time.

5. NUMERICAL RESULTS AND DISCUSSION

For all physical models, the simulations were made for at least three different grids, to allow the determination of apparent convergence order (Marchi, 2001; Marchi and Silva, 2005). Numerical error estimates, also, based on GCI estimator (Roache, 1994), were taken for all physical and chemical models. Some pieces of information about numerical errors and error estimators can be found in Tannehill *et al*. (1997), Marchi (2001), and Ferziger and Perić (2001). Error estimates are very important for evaluating if two different physical (or chemical) models have the same results or the differences can be assigned to numerical errors.

The GCI estimator is evaluated by

$$GCI(\varphi_1, p) = 3\frac{|\varphi_1 - \varphi_2|}{(q^p - 1)} \tag{12}$$

where: φ_1 and φ_2 are, respectively, the numerical solutions for the fine (h_1) and coarse (h_2) grids; q is the grid refinement ratio ($q = h_2 / h_1$); h is the grid spacing or distance between two successive grid points; and p is related to the asymptotic (p_L) or apparent (p_U) order (the lowest value between these two ones). Asymptotic error order depends on the chosen discretization model, while apparent order, for constant refinement ratio, is evaluated by

$$p_U(h_1) = \frac{\log(\psi_U)}{\log(q)} \tag{13}$$

in which ψ_U is the numerical solution convergence ratio for analytical one, defined by

$$\psi_U = \frac{(\varphi_2 - \varphi_3)}{(\varphi_1 - \varphi_2)} \tag{14}$$

where φ_3 corresponds to the numerical solution for a supercoarse grid.

Another error estimators presented in this work are the Richardson estimators, based on asymptotic and on apparent orders (p_L and p_U, respectively), which are defined by the relations:

$$U_{Ri}(\varphi_1, p_L) = \frac{(\varphi_1 - \varphi_2)}{(q^{p_L} - 1)} \tag{15}$$

$$U_{Ri}(\varphi_1, p_U) = \frac{(\varphi_1 - \varphi_2)}{(q^{p_U} - 1)} \tag{16}$$

In the first simulation made, in order to validate the implemented code, constant and variable property models were run for Back *et al*. (1965) nozzle geometry. This flow consists on air flow (gas constant, R, equal to 287.0 J/kg·K and ratio between specific heats, γ, equal to 1.35), with stagnation pressure of 1,725 MPa and stagnation temperature of 833,33 K; for this simulation, CDS-deferred scheme was used, as well as 90x10, 180x20, 360x40 and 720x80 control volume grids (the first value corresponds to axial direction discretization and the second one, to radial direction). Besides the constant air properties flow, also variable properties ones were studied and both results (constant and variable properties), for a 720x80 control volumes grid, are exposed in Fig. 3. Comparing numerical and experimental data, it is seen a good agreement between both results, validating Mach2D code.

Other simulations were made, taking the following values for the parameters: the stagnation pressure and temperature are equal to, respectively, 3,420.33 K and 2.0 MPa; oxidant-fuel mass ratio (OF) is 7.936682739 (stoichoimetrical composition for oxygen and hydrogen reaction); the gas constant (R) is taken as 526.97 J/kg·K; the ratio between specific heats (γ) is equal to 1,1956 (used for constant properties one-species flow). Both interpolation schemes, UDS and CDS with deferred correction, were used, in order to evaluate the apparent order (and the GCI and the Richardson error estimates).

Two-dimensional flow effects are evident by comparing any property distribution at line symmetry and near the walls, as can be seen at Fig. 4 (a), which corresponds to simulations using the Back *et al*. (1965) geometry. It can be seen, also, that differences among near-to-wall results are much smaller than the ones obtained for line symmetry, with the grid refinement. Although Fig. 4 (a) shows only this effect for temperature distribution, other local variables of

interest (such as pressure, Mach number and density distributions) exhibit a similar behaviour. These effects, otherwise, are not observed for global parameters, such as thrust, Fig. 4 (b); for such variables, the differences obtained with the grid refinement are quite small and all the property distributions are nearly coincident. The effects of different physical models (one-species with variable properties, frozen, local equilibrium and non-equilibrium flows) on thrust can be observed in Fig. 5. The frozen and the local equilibrium model results occupy the lowest and the highest limits, respectively. In absolute values, this difference achieves 126,41 N (or nearly 3%, in relative values).

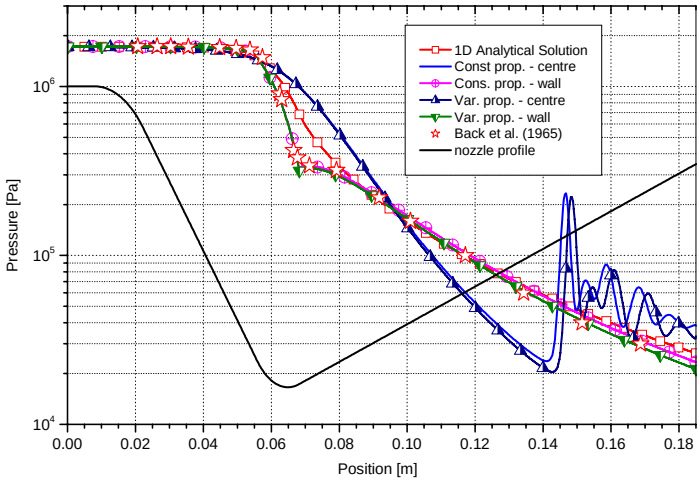

Figure 3. Pressure distribution through the nozzle for air flow (720x80 control volumes).

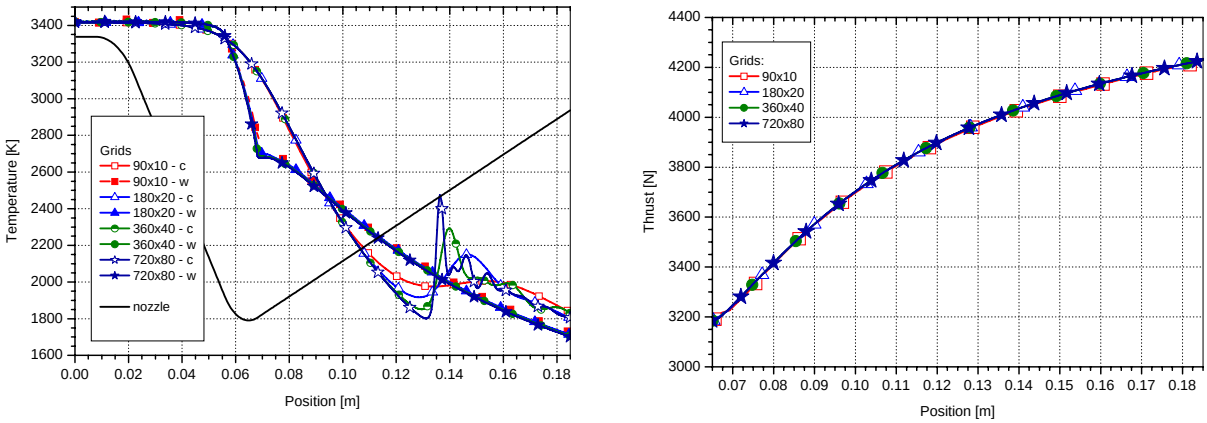

(a) (b)

Figure 4. (a) Temperature distribution and (b) thrust through the nozzle engine (for vacuum conditions), for different grid refinements (frozen flow, chemical model 3, CDS deferred correction interpolation scheme).

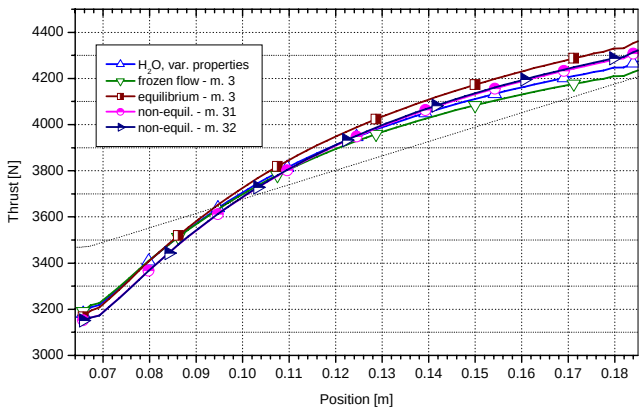

Figure 5. Thrust distribution along the divergent section of the engine, for different chemical models – 90x10 control volumes, geometry of Back *et al*. (1965).

The second geometry used for simulations was the parabolic one, presented in Fig. 2 (b). In order to evaluate the apparent order and the error estimates (by GCI and Richardson estimators), at least 6 different grids were used, for each physical and chemical models studied. To evaluate the influence of the chosen interpolation scheme on the error estimate, both UDS and CDS with deferred correction schemes were employed. For all the simulations, the number of iterations used was enough to assure the achievement of round-off error. For frozen flow and local equilibrium flow models, the tolerances associated to chemical reactions were posed as 10^{-12}, in order to guarantee the convergence for these reaction equations. Apparent order behaviour, for global variables of interest, is shown in Fig. 6, while error estimate, for specific impulse (I_S) is placed in Fig. 7. Both results refer to chemical model 4, for frozen flow and 10x3, 20x6, 40x12, 80x24, 160x48, 320x96 and 640x192 control volume grids.

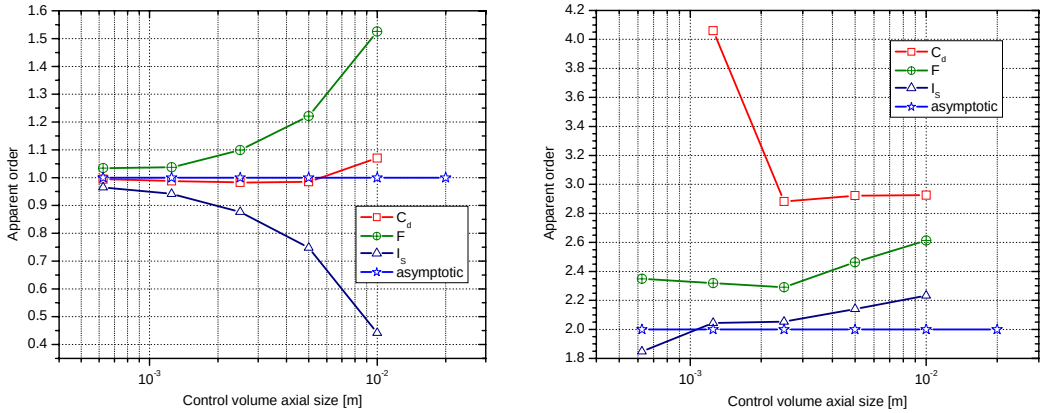

Figure 6. Apparent order obtained for (a) UDS and (b) CDS with deferred correction for model 4, frozen flow.

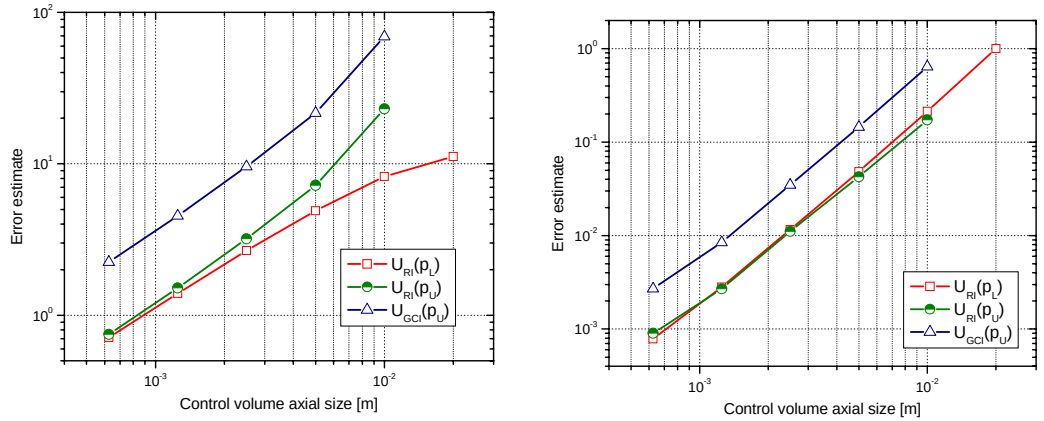

Figure 7. Error estimate for (a) UDS and (b) CDS with deferred correction for I_S (model 4, frozen flow).

Figure 6 shows that the apparent error tends to the asymptotic one when UDS interpolation scheme is employed. For the same grids, however, when CDS scheme is used, this tendency is unclear yet – a greater grid refinement should be needed. Similar behaviour was observed for all the global variables of interest, for the frozen flow model. For local variables of interest (such as exit temperature, exit axial velocity and exit pressure, all of them at line symmetry), the apparent error tendency is unclear, even for UDS scheme. Because of this, more refined grid solutions should be necessary for a correct evaluation of this tendency.

Figure 7 presents the error estimate for Richardson and GCI estimators. GCI estimator always has higher values for error estimate, through its coefficient (which is equal to 3). Despite the unclear tendency for apparent order when CDS scheme is used, error estimates are, at least, three orders-of-magnitude smaller than the ones obtained for UDS scheme, for the 640x192 control volumes grid. Because of this, even if the CDS scheme shows no tendency to achieve the apparent order, its use is recommended, based on the smaller values for error estimate, for frozen flow model.

Figures 8 and 9 refer to local equilibrium flow results. Differently from frozen flow model, apparent order shows a tendency, which is far from the expected value of 2. Even with the study restricted to only 6 grids (10x3, 20x6, 40x12, 80x24, 160x48 and 320x96), both the discharge coefficient and the specific impulse present apparent order values much closer to the unity than to 2. All the terms of the five equations, which model the reactive local equilibrium flow, are

discretized using options that allow the use of both UDS and CDS with deferred correction schemes, expect by the chemical source term, Eq. 6(a). This term is discretized using only UDS scheme and, as it can be seen by the numerical results, its inclusion possibly changes the convergence order of the entire model to first order, even though it is still over the unity value for the 320x96 grid, for thrust and specific impulse. Because of this, error estimate for both UDS and CDS with deferred correction present only a one-order-of-magnitude difference, in spite of 3 as verified for frozen flow model, as can be seen in Fig. 9.

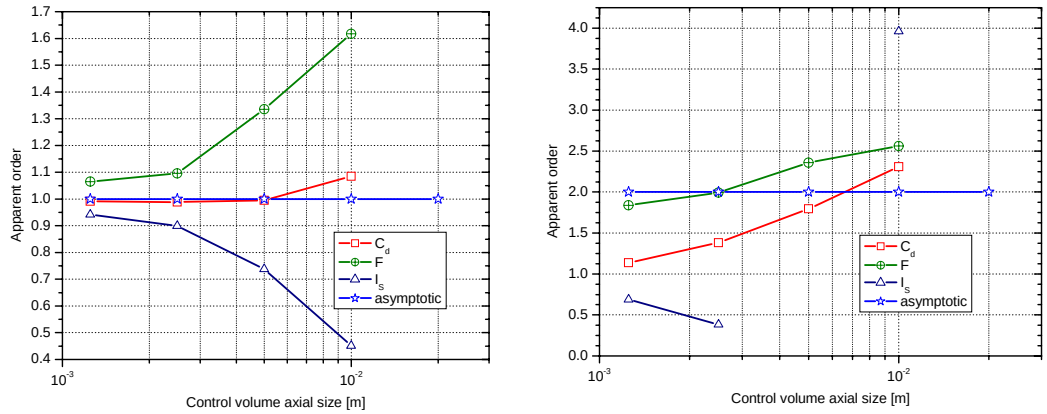

Figure 8. Apparent order obtained for (a) UDS and (b) CDS with deferred correction for model 4, equilibrium flow.

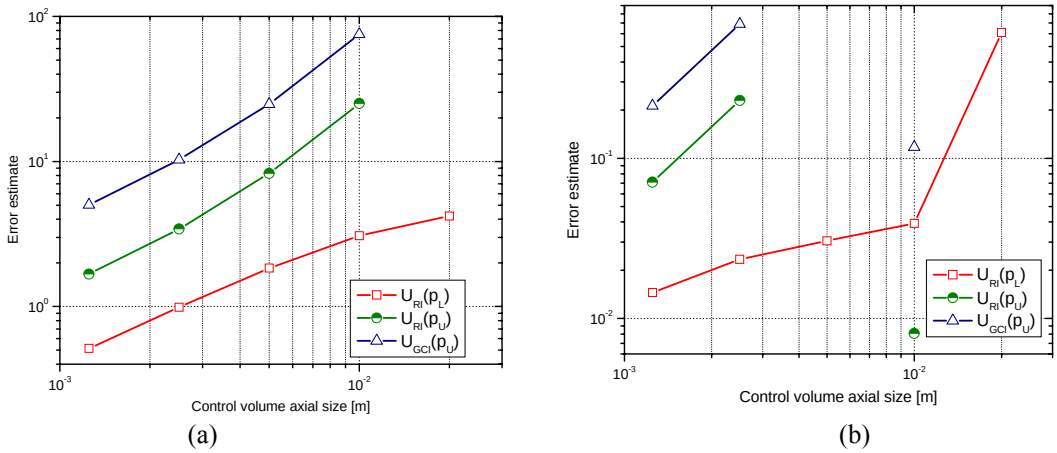

Figure 9. Error estimate for (a) UDS and (b) CDS with deferred correction for I_S (model 4, equilibrium flow).

Comparisons of physical and chemical models, as well as for UDS and CDS with deferred correction interpolation schemes, are presented at Tables 2 and 3. For all results, GCI error estimates were obtained, except for H_2O-exit-mass-fraction for frozen models, because of the constancy of these values all over the flow. Kliegel and Levine (1969) provide an analytical solution for the discharge coefficient: their hypotheses include a perfect gas flow with constant properties – which corresponds to one-species, constant properties model. The numerical results ranges, obtained using the Mach2D code, for both UDS and CDS schemes, include this analytical solution. It can be noted, however, that the numerical error estimate associated to CDS scheme is, at least, three orders-of-magnitude lower than those ones obtained for UDS scheme. Similar behaviour is observed for all physical and chemical models and for all variables of interest. The advantage of CDS scheme is smaller only for local equilibrium flow model, for which the convergence order tends to the unity value.

Differences between physical models are quite small for all global variables of interest: it corresponds only to 2.3% for discharge coefficient, 2.7% for thrust and 5.1% for specific impulse. For local variables, otherwise, these differences are more appreciable: 20.4% for exit pressure and 37.9% for exit temperature (at line symmetry). Axial exit velocity, otherwise, is nearly not affect by the physical model, once the difference between the extreme values is about only 2.4%. Six and eight chemical species models have similar results, which are, for many variables, numerically identical, once the error estimate ranges are the same. The CPU time required, however, are different, specially for local equilibrium flow: while model 4 demanded 13.6 hours for 30,000 iterations, model 10 needed 21.3 hours (57.3% more), for the same number of iterations.

Table 2. Results for discharge coefficient, thrust and specific impulse, for the parabolic nozzle (320x96 grid).

Model	C_d [adim.]	F [N]	I_S [s]
UDS			
One-species, constant properties	$1.01 \pm 2\text{x}10^{-2}$	$1.628\text{x}10^{4} \pm 8\text{x}10^{1}$	$3.45\text{x}10^{2} \pm 5\text{x}10^{0}$
One-species, variable properties	$1.00 \pm 2\text{x}10^{-2}$	$1.635\text{x}10^{4} \pm 8\text{x}10^{1}$	$3.45\text{x}10^{2} \pm 5\text{x}10^{0}$
Frozen Flow – mod. 4	$1.01 \pm 2\text{x}10^{-2}$	$1.621\text{x}10^{4} \pm 9\text{x}10^{1}$	$3.39\text{x}10^{2} \pm 5\text{x}10^{0}$
Frozen Flow – mod. 10	$1.01 \pm 2\text{x}10^{-2}$	$1.621\text{x}10^{4} \pm 8\text{x}10^{1}$	$3.39\text{x}10^{2} \pm 5\text{x}10^{0}$
Equilibrium Flow – mod. 4	$0.98 \pm 1\text{x}10^{-2}$	$1.665\text{x}10^{4} \pm 7\text{x}10^{1}$	$3.56\text{x}10^{2} \pm 5\text{x}10^{0}$
Equilibrium Flow – mod. 10	$0.98 \pm 2\text{x}10^{-2}$	$1.665\text{x}10^{4} \pm 7\text{x}10^{1}$	$3.56\text{x}10^{2} \pm 5\text{x}10^{0}$
CDS with deferred correction			
One-species, constant properties	$0.999876 \pm 2\text{x}10^{-6}$	$1.62516\text{x}10^{4} \pm 4\text{x}10^{-1}$	$3.41743\text{x}10^{2} \pm 8\text{x}10^{-3}$
One-species, variable properties	$0.991678 \pm 4\text{x}10^{-6}$	$1.632442\text{x}10^{4} \pm 8\text{x}10^{-2}$	$3.46111\text{x}10^{2} \pm 3\text{x}10^{-3}$
Frozen Flow – mod. 4	$1.000962 \pm 2\text{x}10^{-6}$	$1.61859\text{x}10^{4} \pm 4\text{x}10^{-1}$	$3.39993\text{x}10^{2} \pm 8\text{x}10^{-3}$
Frozen Flow – mod. 10	$1.000970 \pm 2\text{x}10^{-6}$	$1.61860\text{x}10^{4} \pm 4\text{x}10^{-1}$	$3.39991\text{x}10^{2} \pm 8\text{x}10^{-3}$
Equilibrium Flow – mod. 4	$0.9785 \pm 4\text{x}10^{-4}$	$1.6625\text{x}10^{4} \pm 1\text{x}10^{0}$	$3.572\text{x}10^{2} \pm 2\text{x}10^{-1}$
Equilibrium Flow – mod. 10	$0.9785 \pm 4\text{x}10^{-4}$	$1.6625\text{x}10^{4} \pm 1\text{x}10^{0}$	$3.572\text{x}10^{2} \pm 2\text{x}10^{-1}$
Kliegel and Levine (1969) – analytical solution 2D	**0.999877**	---	---

Table 3. Results for exit pressure, exit temperature, exit axial velocity and exit H_2O mass fraction (all of them for line symmetry), for the parabolic nozzle (320x96 grid).

Model	P_{ex} [Pa]	T_{ex} [K]	u_{ex} [m/s]	$Y(H_2O)_{ex}$ [adim.]
UDS				
One-species, constant properties	$7.2\text{x}10^{4} \pm 7\text{x}10^{3}$	$1.99\text{x}10^{3} \pm 4\text{x}10^{1}$	$3.03\text{x}10^{3} \pm 5\text{x}10^{1}$	---
One-species, variable properties	$7\text{x}10^{4} \pm 1\text{x}10^{4}$	$2.09\text{x}10^{3} \pm 4\text{x}10^{1}$	$3.06\text{x}10^{3} \pm 6\text{x}10^{1}$	---
Frozen Flow – mod. 4	$6.9\text{x}10^{4} \pm 3\text{x}10^{3}$	$1.92\text{x}10^{3} \pm 3\text{x}10^{1}$	$3.03\text{x}10^{3} \pm 5\text{x}10^{1}$	0.783686
Frozen Flow – mod. 10	$6.9\text{x}10^{4} \pm 2\text{x}10^{3}$	$1.92\text{x}10^{3} \pm 3\text{x}10^{1}$	$3.03\text{x}10^{3} \pm 4\text{x}10^{1}$	0.783539
Equilibrium Flow – mod. 4	$8.3\text{x}10^{4} \pm 3\text{x}10^{3}$	$2.64\text{x}10^{3} \pm 1\text{x}10^{1}$	$3.10\text{x}10^{3} \pm 5\text{x}10^{1}$	$0.902 \pm 2\text{x}10^{-3}$
Equilibrium Flow – mod. 10	$8.3\text{x}10^{4} \pm 2\text{x}10^{3}$	$2.64\text{x}10^{3} \pm 1\text{x}10^{1}$	$3.10\text{x}10^{3} \pm 5\text{x}10^{1}$	$0.902 \pm 2\text{x}10^{-3}$
CDS with deferred correction				
One-species, constant properties	$7.14\text{x}10^{4} \pm 9\text{x}10^{2}$	$1.98\text{x}10^{3} \pm 1\text{x}10^{1}$	$3.04\text{x}10^{3} \pm 2\text{x}10^{1}$	---
One-species, variable properties	$7.34\text{x}10^{4} \pm 9\text{x}10^{2}$	$2.083\text{x}10^{3} \pm 7\text{x}10^{0}$	$3.07\text{x}10^{3} \pm 1\text{x}10^{1}$	---
Frozen Flow – mod. 4	$6.90\text{x}10^{4} \pm 9\text{x}10^{2}$	$1.91\text{x}10^{3} \pm 2\text{x}10^{1}$	$3.04\text{x}10^{3} \pm 5\text{x}10^{1}$	0.783686
Frozen Flow – mod. 10	$6.90\text{x}10^{4} \pm 9\text{x}10^{2}$	$1.91\text{x}10^{3} \pm 2\text{x}10^{1}$	$3.04\text{x}10^{3} \pm 5\text{x}10^{1}$	0.783539
Equilibrium Flow – mod. 4	$8.31\text{x}10^{4} \pm 8\text{x}10^{2}$	$2.6345\text{x}10^{3} \pm 1\text{x}10^{-1}$	$3.113\text{x}10^{3} \pm 5\text{x}10^{0}$	$0.9028 \pm 7\text{x}10^{-4}$
Equilibrium Flow – mod. 10	$8.31\text{x}10^{4} \pm 8\text{x}10^{2}$	$2.6347\text{x}10^{3} \pm 1\text{x}10^{-1}$	$3.113\text{x}10^{3} \pm 5\text{x}10^{0}$	$0.9027 \pm 9\text{x}10^{-4}$

6. CONCLUSION

A two-dimensional code, for chemical reaction flows where implemented, using Fortran 95 language and Visual Compaq 6.6.0 compiler. Five physical models were studied: a one-species flow (with constant or with variable properties); and the other three for reaction gas products (frozen, local equilibrium and non-equilibrium flows). For frozen and equilibrium models, nine different chemical reaction schemes were implemented – the same chemical reaction schemes discussed by Marchi *et al*. (2005) –, but only two were studied. Two nozzle geometries were used – one presented in the work of Back *et al*. (1965) and the other is a parabolic one. Numerical solutions for air flow were compared to the ones presented in the first work, with good agreement. Two-dimensional discharge coefficient values for one-species flow were compared to the two-dimensional analytical solution provided by Kliegel and Levine (1969), also showing good concordance.

Apparent convergence order, as well as Richardson and GCI estimators were obtained for the parabolic geometry simulations. Both UDS and CDS with deferred correction schemes were employed, and their results (including error estimates) were compared. Because of the discretization of the chemical source-term in energy equation by UDS scheme, the whole local equilibrium model seems to be of first order of convergence, even when CDS scheme is used. Because of this, also, the difference between UDS and CDS for the error estimate order of magnitude is lower for local equilibrium model. While this difference can be as high as four orders of magnitude for other physical models (for global variables of interest), it achieves only two orders of magnitude for local equilibrium models.

7. ACKNOWLEDGEMENTS

The authors would acknowledge Federal University of Paraná (UFPR), Coordenação de Aperfeiçoamento de Pessoal de Nível Superior (CAPES) and The "UNIESPAÇO Program" of The Brazilian Space Agency (AEB) by physical and financial support given for this work. The first author would, also, acknowledge his professors and friends, by discussions and other forms of support. The second author is scholarship of CNPq (Conselho Nacional de Desenvolvimento Científico e Tecnológico) – Brazil.

8. REFERENCES

Araki, L. K., Marchi, C. H., 2006, "Numerical Solution of an One-Dimensional Reactive Flow in a Regeneratively Rocket Engine Nozzle", Proceedings of the 11th Brazilian Congress of Thermal Sciences and Engineering, ABCM, Curitiba, Brazil.

Back, L. H., Massier, P. F., Gier, H. L., 1965, "Comparison of measured and predicted flows through conical supersonic nozzles, with emphasis on the transonic region", AIAA Journal, Vol. 3, N. 9, pp. 1606-1614.

Barros, J. E. M., Alvim Filho, G. F., Paglione, P., 1990, "Estudo de Escoamento Reativo em Desequilíbrio Químico através de Bocais Convergente Divergente", Proceedings of the III Encontro Nacional de Ciências Térmicas, ABCM, Itapema, Brazil.

Ferziger, J. H., Perić, M., 2001, "Computational Methods for Fluid Dynamics", 3ed., Berlin: Springer-Verlag.

Fröhlich, A., Popp, M., Schmidt, G., Thelemann, D., 1993, "Heat Transfer Characteristics of H_2/O_2 Combustion Chambers", Proceedings of the 29th Joint Propulsion Conference, Monterrey, USA, AIAA 93-1826.

Habiballah, M., Vingert, L., Vuillermoz, P., 1998, "Research as a Key in the Design Methodology of Liquid-Propellant Combustion Devices", Journal of Propulsion and Power, V.14, N. 5, pp. 782-788.

Huzel, D. K., Huang, D. H., 1992, "Modern Engineering for Design of Liquid-Propellant Rocket Engines", AIAA Progress in Astronautics and Aeronautics.

Kee, R. J., GrCar, J. F., Smooke, M. D, Miller, J. A., 1990, "A Fortran Program for Modeling Steady Laminar One-Dimensional Premixed Flames", Albuquerque: Sandia National Laboratories, SAND85-8240•UC-401.

Kliegel, J. R., Levine, J. N., 1969, "Transonic flow in small throat radius of curvature nozzle", AIAA Journal, Vol. 7, pp. 1375-1378.

Maliska, C. R., 1995, "Transferência de Calor e Mecânica dos Fluidos Computacional", Rio de Janeiro, LTC Editora.

Marchi, C. H., 2001, "Verificação de Soluções Numéricas Unidimensionais em Dinâmica dos Fluidos", Thesis (Mechanical Engineering PhD). Universidade Federal de Santa Catarina, Florianópolis, SC.

Marchi, C. H., Araki, L. K., Laroca, F., 2005, "Evaluation of Thermochemical Properties and Combustion Temperatures for LOX/LH_2 Reaction Schemes", Proceedings of the 26th Iberian Latin-American Congress on Computational Methods in Engineering, ABCM, Guarapari, Brazil.

Marchi, C. H., Laroca, F., Silva, A. F. C., Hinckel, J. N., 2004, "Numerical Solutions of Flows in Rocket Engines with Regenerative Cooling", Numerical Heat Transfer, *Part A*, Vol.45, pp. 699-717.

Marchi, C. H., Maliska, C. R., 1994, "A nonorthogonal finite volume method for the solution of all speed flows using co-located variables", Numerical Heat Transfer*, Part B*, v. 26, pp. 293 – 311.

Marchi, C. H., Silva, A. F. C., 2005, "Multi-dimensional Discretization Error Estimation for Convergent Apparent Order", Journal of the Brazilian Society of Mechanical Sciences and Engineering, Vol. 27, N. 4, pp. 432-439.

Roache, P. J., 1994, "Persperctive: A method for uniform reporting of grid refinement studies", Journal of Fluids Engineering, Vol. 116, pp. 405-413.

Schneider, G. E., Zedan, M., 1981, "A Modified Strongly Implicit Procedure for the Numerical Solution of Field Problems", Numerical Heat Transfer, v. 4, pp. 1-19.

Smith, T. A., Pavli, A. J., Kacynski, K. J., 1987, "Comparison of Theoretical and Experimental Thrust Performance of a 1030:1 Area Ratio Rocket Nozzle at a Chamber Pressure of 2413 kN/m^2 (350 psia)", Cleveland, NASA Lewis Research Center, NASA Technical Paper 2725.

Sutton, G. P., Biblarz, O, 2001, "Rocket Propulsion Elements", 7 ed., New York, John Willey & Sons.

Svehla, R. A., 1964, "Thermodynamic and Transport Properties for the Hydrogen-Oxygen System", Cleveland, NASA Lewis Center, NASA SP-3011.

Tanehill, J. C., Anderson, D., Pletcher, R. H., 1997, "Computational Fluid Mechanics and Heat Transfer", 2ed., Philadelphia: Taylor & Francis.

Van Doormal, J. P., Raithby, G. D., 1984, "Enhancements of the SIMPLE method for predicting incompressible fluid flow", Numerical Heat Transfer, v. 7, pp. 147-163.

9. RESPONSIBILITY NOTICE

The authors are the only responsible for the printed material included in this paper.